DQ Analysis of 3D Natural Convection in an Inclined Cavity using an Velocity-Vorticity Formulation

D. C. Lo, and S. S. Leu

Abstract—In this paper, the differential quadrature method is applied to simulate natural convection in an inclined cubic cavity using velocity-vorticity formulation. The numerical capability of the present algorithm is demonstrated by application to natural convection in an inclined cubic cavity. The velocity Poisson equations, the vorticity transport equations and the energy equation are all solved as a coupled system of equations for the seven field variables consisting of three velocities, three vorticities and temperature. The coupled equations are simultaneously solved by imposing the vorticity definition at boundary without requiring the explicit specification of the vorticity boundary conditions. Test results obtained for an inclined cubic cavity with different angle of inclinations for Rayleigh number equal to 10^3, 10^4, 10^5 and 10^6 indicate that the present coupled solution algorithm could predict the benchmark results for temperature and flow fields. Thus, it is convinced that the present formulation is capable of solving coupled Navier-Stokes equations effectively and accurately.

Keywords—Natural convection, velocity-vorticity formulation, differential quadrature (DQ).

I. INTRODUCTION

COMPUTATION of incompressible Navier-Stokes equations is an important area in CFD related fields in science and engineering. With the development of a wide range of numerical schemes and algorithms, obtaining numerical solution of the Navier-Stokes equations now has become much easier compared to the previous decades. However, there is a continuous research going on in the development of new numerical algorithms as the CFD is being used as a modeling tool in other areas of science as well. The velocity-vorticity formulation, pioneered by Fasel [1] is considered to be an alternate form of the Navier-Stokes equations without involving the pressure term.

Generally the vorticity boundary values are determined explicitly using a second order accurate Taylor's series expansion scheme while computing flow fields using the velocity-vorticity form of the Navier-Stokes equations. Hence

care must be taken to assure accurate computation of the vorticity values at the boundaries by using finer mesh near the boundaries when lower order schemes are used for vorticity definition. The use of the differential quadrature method enables the computation of vorticity definition with higher order polynomials. Furthermore, when a coupled numerical scheme involving a global method of differential quadrature (DQ) method is used to solve the governing equations, the explicit specification of vorticity definition at the boundary is completely eliminated, resulting in a simplified computational procedure.

The DQ method was first pioneered by Bellman et al. [2] to approximate the derivative of a smooth function and has been successfully implemented for solving many engineering problems [3]. The present study proposes a novel idea to solve three-dimensional Navier-Stokes equations by efficiently exploiting the advantages of both the velocity-vorticity form of the Navier-Stokes equations and the DQ method. Natural convection in a differentially heated inclined cubic cavity is represented by continuity equation, momentum equations and energy equation, which are coupled due to the buoyancy term appearing in the momentum equation. Hence natural convection in an inclined cubic cavity is considered to be the best example problem to test the numerical capability of the proposed coupled algorithm. All the seven field variables involving three velocities, three vorticities and temperature are solved using a single global matrix as a coupled system of variables.

The proposed numerical scheme is applied to determine the velocity, vorticity and temperature variations for natural convection problem in a differentially heated inclined cubic cavity for Rayleigh number range from 10^3 to 10^6. Numerical formulation, solution procedure and comparisons of the present results with those obtained by other numerical schemes are presented in the following sections.

II. DIFFERENTIAL QUADRATURE METHOD

The DQ method replaces a given spatial derivative of a function $f(x)$ by a linear weighted sum of the function values at the discrete sample points considered along a coordinate direction, resulting in a set of algebraic equations. Hence the DQ method can be used to obtain numerical solution of partial differential equations with higher order accuracy. For a function of three variables $f(x, y, z)$, the p th order

World Academy of Science, Engineering and Technology
International Journal of Mathematical and Computational Sciences
Vol:2, No:10, 2008

derivatives, q th order derivatives and r th order derivatives of the function with respect to x, y and z coordinates can be obtained as:

$$f_x^{(p)}(x_i, y_j, z_k) = \sum_{l=1}^{L} A_{i,l}^{(p)} f(x_l, y_j, z_k), p = 1, 2, ..., L-1 \qquad (1)$$

$$f_y^{(q)}(x_i, y_j, z_k) = \sum_{m=1}^{M} B_{j,m}^{(q)} f(x_i, y_m, z_k), q = 1, 2, ..., M-1 \qquad (2)$$

$$f_z^{(r)}(x_i, y_j, z_k) = \sum_{n=1}^{N} C_{k,n}^{(r)} f(x_i, y_j, z_n), r = 1, 2, ..., N-1 \qquad (3)$$

for $i = 1, 2, ..., L$; $j = 1, 2, ..., M$; $k = 1, 2, ..., N$

where l, m, n are the indices for the grid points in the x, y and z coordinates respectively, L, M, N are the number of grid points in the x, y and z directions respectively and $A_{i,l}^{(p)}, B_{j,m}^{(q)}, C_{k,n}^{(r)}$ are the weighting coefficients. The first order weighting coefficients $A_{i,l}^{(1)}, B_{j,m}^{(1)}, C_{k,n}^{(1)}$ can be determined as follows:

$$A_{i,j}^{(1)} = \frac{L^{(1)}(x_i)}{(x_i - x_j)L^{(1)}(x_j)}, i, j = 1, 2, ..., L, \quad but \ j \neq i \qquad (4)$$

$$B_{i,j}^{(1)} = \frac{M^{(1)}(y_i)}{(y_i - y_j)M^{(1)}(y_j)}, i, j = 1, 2, ..., M, \quad but \ j \neq i \qquad (5)$$

$$C_{i,j}^{(1)} = \frac{N^{(1)}(z_i)}{(z_i - z_j)N^{(1)}(z_j)}, i, j = 1, 2, ..., N, \quad but \ j \neq i \qquad (6)$$

in which

$$L^{(1)}(x_i) = \prod_{j=1, j \neq i}^{L} (x_i - x_j),$$

$$M^{(1)}(y_i) = \prod_{j=1, j \neq i}^{M} (y_i - y_j),$$

$$N^{(1)}(z_i) = \prod_{j=1, j \neq i}^{N} (z_i - z_j)$$

Similarly the weighting coefficients for the second-and higher-order derivatives can be obtained as

$$A_{i,j}^{(p)} = p(A_{i,i}^{(p-1)} A_{i,j}^{(1)} - \frac{A_{i,j}^{(p-1)}}{x_i - x_j}), \qquad (7)$$

$$i, j = 1, 2, ..., L, \quad but \ j \neq i, l = 2, 3, ..., L-1$$

$$B_{i,j}^{(q)} = q(B_{i,i}^{(q-1)} B_{i,j}^{(1)} - \frac{B_{i,j}^{(q-1)}}{y_i - y_j}), \qquad (8)$$

$$i, j = 1, 2, ..., M, \quad but \ j \neq i, m = 2, 3, ..., M-1$$

$$C_{i,j}^{(r)} = r(C_{i,i}^{(r-1)} C_{i,j}^{(1)} - \frac{C_{i,j}^{(r-1)}}{z_i - z_j}), \qquad (9)$$

$$i, j = 1, 2, ..., N, \quad but \ j \neq i, n = 2, 3, ..., N-1$$

It should be noted from the above equations that the weighting coefficients of the second and higher-order derivatives can be computed from the first-order derivatives themselves.

III. GOVERNING EQUATIONS

The governing equations for natural convection can be described by the incompressible Navier-Stokes equations and the energy equation. Assuming the Boussinesq approximation, the velocity-vorticity form of the Navier-Stokes equations can be written in non-dimensional form as follows:

Velocity Poisson equations

$$\nabla^2 u = -\nabla \times \vec{\omega} \qquad (10)$$

Vorticity transport equations

$$\frac{\partial \vec{\omega}}{\partial t} + (\vec{v} \cdot \nabla)\vec{\omega} = (\vec{\omega} \cdot \nabla)\vec{v} + Pr \cdot \nabla^2 \vec{\omega} - Ra Pr \nabla \times T\vec{g} \qquad (11)$$

Energy equation

$$\frac{\partial T}{\partial t} + (\vec{v} \cdot \nabla)T = \nabla^2 T \qquad (12)$$

The computational domain is discretized using a Cartesian coordinate frame with $x - y$ representing the horizontal plane and z directing in the vertical direction. In the velocity-vorticity form of the Navier-Stokes equations, the vorticity vector is defined as

$$\vec{\omega} = \nabla \times \vec{u} \qquad (13)$$

Equations (10-12) are the final form of the governing equations that characterize the flow and heat transfer during a natural convection process. These equations have to be solved in a computational domain Ω which is enclosed by a solid boundary Γ. For the problem of natural convection in a differentially heated cubic cavity, no-slip velocity boundary conditions are assumed on all the boundary walls.

IV. NUMERICAL SOLUTION

Application of the DQ method to spatial discretization of the governing equations results in a set of algebraic equations. For example, the velocity Poisson equation in the $x - direction$ is approximated using the DQ method to obtain the velocity component in the one coordinate direction as follows,

$$\sum_{l=1}^{L} A_{i,l}^{(2)} u_{l,j,k} + \sum_{m=1}^{M} B_{j,m}^{(2)} u_{i,m,k} + \sum_{n=1}^{N} C_{k,n}^{(2)} u_{i,j,n}$$
$$+ \sum_{m=1}^{M} B_{j,m}^{(1)} \varsigma_{i,m,k} - \sum_{n=1}^{N} C_{k,n}^{(1)} \eta_{i,j,n} = 0 \qquad (14)$$

Similarly, the velocity components in the $y-$, $z - directions$ also can be used the same formulas.

The time derivatives of the convection-diffusion equation (vorticity transport equations and energy equation) are discretized using a second order accurate three-time-level scheme expressed as

$$\frac{\partial \phi}{\partial t} + \vec{v} \cdot \nabla \phi = \nabla^2 \phi + f \Rightarrow \qquad (15)$$
$$\frac{3\phi^{t+1} - 4\phi^t + \phi^{t-1}}{2\Delta t} + 2\vec{v}^t \cdot \nabla \phi^t - \vec{v}^{t-1} \cdot \nabla \phi^{t-1} = \nabla^2 \phi^{t+1} + f^{t+1}$$

The convection-diffusion equation (15) is approximated by the DQ method as follows:

World Academy of Science, Engineering and Technology
International Journal of Mathematical and Computational Sciences
Vol:2, No:10, 2008

$$\frac{(3\phi_{i,j,k}^{t+1})}{2\Delta t} - \left(\sum_{l=1}^{L} A_{i,l}^{(2)}\phi_{l,j,k} + \sum_{m=1}^{M} \phi_{j,m}^{(2)}\xi_{i,m,k} + \sum_{n=1}^{N} C_{k,n}^{(2)}\phi_{i,j,n}\right)^{t+1} - (f_{i,j,k}^{t+1})$$

$$= \frac{(4\phi_{i,j,k}^{t})}{2\Delta t} - \frac{(\phi_{i,j,k}^{t-1})}{2\Delta t}$$

$$-2(u_{i,j,k}\sum_{l=1}^{L} A_{i,l}^{(1)}\phi_{l,j,k} + v_{i,j,k}\sum_{m=1}^{M} B_{j,m}^{(1)}\phi_{i,m,k} + w_{i,j,k}\sum_{n=1}^{N} C_{k,n}^{(1)}\phi_{i,j,n})^{t}$$

$$+(u_{i,j,k}\sum_{l=1}^{L} A_{i,l}^{(1)}\phi_{l,j,k} + v_{i,j,k}\sum_{m=1}^{M} B_{j,m}^{(1)}\phi_{i,m,k} + w_{i,j,k}\sum_{n=1}^{N} C_{k,n}^{(1)}\phi_{i,j,n})^{t-1}$$

(16)

Using the above formula, the vorticity transport equations in the $x-$, $y-$, $z-$ directions and energy equation can be adopted the above method of approximation.

In the successive time step, we used the velocity, vorticity and temperature components at the previous time step as the initial guess for the next iteration. The computations are carried out until steady state conditions are reached. The convergence criteria used in the time loop to achieve steady state conditions are

$$\left|(u^{t+1}-u^t)/u^t\right| \le 10^{-6}, \left|(v^{t+1}-v^t)/v^t\right| \le 10^{-6}, \left|(w^{t+1}-w^t)/w^t\right| \le 10^{-6}$$

$$\left|(\xi^{t+1}-\xi^t)/\xi^t\right| \le 10^{-6}, \left|(\eta^{t+1}-\eta^t)/\eta^t\right| \le 10^{-6}, \left|(\zeta^{t+1}-\zeta^t)/\zeta^t\right| \le 10^{-6}$$ (17)

$$\left|(T^{t+1}-T^t)/T^t\right| \le 10^{-6}$$

TABLE I
GRID-INDEPENDENCE STUDY RESULTS FOR $Ra = 10^4, 10^5, 10^6$

Grids	Nu	$Ra = 10^4$	$Ra = 10^5$	$Ra = 10^6$
PSC [4]	Nu_{mean}	2.2505	4.6127	8.8771
81^3 grids	Nu_{over}	2.0542	4.3371	8.6407
Present	Nu_{mean}	2.2532	4.6238	8.9091
21^3 grids	Nu_{over}	2.0521	4.3287	8.6691
Present	Nu_{mean}	2.2507	4.6103	8.9096
23^3 grids	Nu_{over}	2.0541	4.3352	8.6681
Present	Nu_{mean}	2.2507	4.6103	8.9096
25^3 grids	Nu_{over}	2.0541	4.3352	8.6681
Present	Nu_{mean}	2.2507	4.6103	8.9096
31^3 grids	Nu_{over}	2.0541	4.3352	8.6681

V. NUMERICAL RESULTS

The schematic diagram of the inclined cubic cavity with the boundary conditions for the natural convection problem is displayed in Fig. 1. Temperatures equal to –0.5 and 0.5 are enforced on the left wall at $x = -0.5$ and the right wall at $x = 0.5$ respectively. Numerical results obtained for the test problem are discussed in this section.

A. Grid Independence Study

One of the aims of the present numerical scheme is to show that the use of higher order polynomials for approximating the partial differential equations requires relatively a coarse mesh

to achieve benchmark solutions. In order to validate the computer program developed to solve the governing equations for the natural convection problem, initially a grid independence study was carried out for $Ra = 10^4, 10^5, 10^6$.

Further, in order to make sure that the grid independence study is in accordance with other numerical results, the grid independence study results obtained for the case of $\phi = 0$ were compared with the results of Tric et al. [4] who used pseudo-spectral Chebyshev algorithm based on the projection-diffusion method with a spatial resolution supplied by polynomial expansions. For the mesh sensitivity study, the mean and the overall Nusselt number values were computed for $10^4 \le Ra \le 10^6$ using four different meshes. The value of Prandtl number was assumed as 0.71 for all these computations. Table I depicts the comparisons between the values of the mean and the overall Nusselt numbers obtained using the present method for the four mesh sizes and the results obtained by Tric et al. [4]. It can be observed that the results obtained by using the present numerical algorithm with the above four grids of size are almost in excellent agreement with the results of Tric et al. [4] for all the values of the Rayleigh numbers considered in this study.
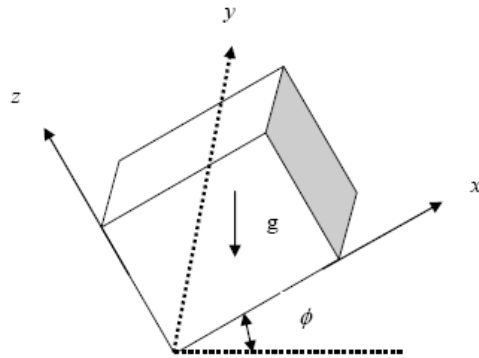

Fig. 1 Layout of the problem

B. Effect of Angle of Inclination on Natural Convection Phenomenon References

In order to capture the three-dimensional effect of the temperature fields, the temperature variations on the mid-planes along the principal axes serve as a visual representation of the temperature variations throughout the cavity due to the buoyancy-induced flows. Figs. 2(a) to 2(d) show the temperature contours on $x-z$ plane at $y = 0.5$ for different angles of inclination for $Ra = 10^5$. As far as the convective heat transport is concerned this is the principal plane that indicates the heat transfer phenomena because this plane consists of the axes of the temperature differentials and the gravitational direction. The temperature maps are very close to the hot and the cold walls compared to the other sides, because greater temperature gradients are observed only at these regions. As the other sides are kept adiabatic, the temperature contours are always normal to these sides as observed in the above figures. Further the increase in the angle

World Academy of Science, Engineering and Technology
International Journal of Mathematical and Computational Sciences
Vol:2, No:10, 2008

of inclination results in diagonally parallel isotherms instead of the nearly horizontal isotherms observed at $\phi = 0°$.

Apart from testing the code for the present formulation with respect to the Nusselt numbers, it is also required to verify for the flow fields. The characteristics of the natural convection phenomenon can be well understood by plotting the velocity vectors on the various symmetric mid-planes along the principal axes. Figs. 3(a), 3(b) represent the velocity vectors plotted on $x - z$ plane at $y = 0.5$ symmetric plane of the cavity for $\phi = 0°, 30°$, respectively at $Ra = 10^5$. As the angle of inclination increases the effect of decreased buoyancy forces is felt on the flow pattern. With increase in the angle of inclination, the velocity gradient decreases near the vertical walls as observed in the above figures.

TABLE II
NUMERICAL RESULTS FOR $Ra = 10^4, 10^5, 10^6$ AT DIFFERENT ANGLES

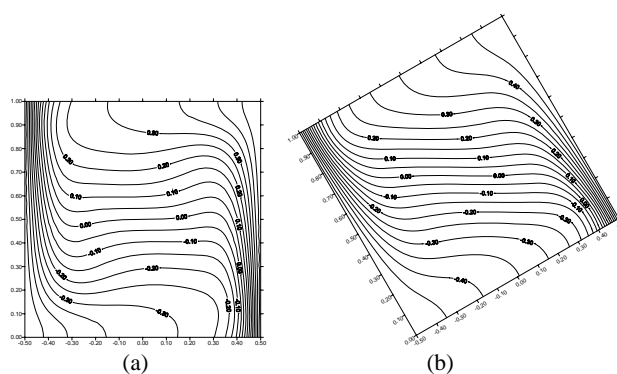| ϕ	Ra	Nu_{mean}	Nu_{over}
0°	10^4	2.2507	2.0541
15°		1.9858	1.8425
30°		1.6800	1.5894
45°		1.3913	1.3434
60°		1.1720	1.1524
75°		1.0331	1.0377
90°		1.0152	1.0152
0°	10^5	4.6103	4.3352
15°		3.9690	3.7731
30°		3.0241	2.9014
45°		2.0385	1.9791
60°		1.3840	1.3623
75°		1.0367	1.0789
90°		1.1603	1.1603
0°	10^6	8.9096	8.6681
15°		7.5445	7.3630
30°		5.3303	5.2133
45°		2.8754	2.8202
60°		1.5829	1.5585
75°		1.0084	1.1184
90°		1.8237	1.8237

The capability of the present numerical scheme can be tested by plotting the vorticity contours at the $y = 0.5$ plane as shown in Fig. 4 for different angles of inclination for $Ra = 10^5$. As the angle of inclination increases, the buoyancy force is not sufficient enough to generate the convective current of the fluid. Hence the expected increased fluid convection due to decrease in the angle of inclination.

Nusselt number is an important non-dimensional parameter in convective heat transfer study. The mean value of the Nusselt number computed for the isothermal walls are shown as variations along the $y -$ direction in Figs. 5(a) to 5(d) for $Ra = 10^3, 10^4, 10^5, 10^6$ respectively. Also, Table II shows the comparison of the mean value and overall value of the Nusselt number for $Ra = 10^4, 10^5, 10^6$ at different angles. An initial look on the range of the Nusselt number values shown on these figures clearly indicates that the Nusselt number increases with increase in the value of the Rayleigh number as expected. A symmetric variation is observed in all these figures. However the number of peaks and their positions vary with the value of the Rayleigh number. The maximum value of the Nusselt number is achieved only for $\phi = 0°$ as expected. As the angle of inclination increases, the maximum value of the Nusselt number decreases as seen from these figures for the cases of $Ra = 10^3, 10^4, 10^5$. The results discussed for the inclined cavity demonstrate that the present numerical algorithm has correctly predicted the convective heat transport process inside the cavity for different values of angle of inclination. The proposed algorithm could enforce the vorticity boundary values implicitly. This fact is verified by the expected results predicted by the present algorithm for the flow and the temperature fields.

VI. CONCLUSION

A coupled numerical algorithm proposed based on the velocity-vorticity formulation and the DQ method was tested for natural convection in a differentially heated inclined cubic cavity. Test results obtained for Rayleigh number in the range from 10^3 to 10^6 at the angle of incidence ($\phi = 0°$) show close agreements with other numerical scheme, producing the expected flow and temperature fields. Moreover, the salient characteristics of the different angle of incidence, $0° \leq \phi \leq 90°$ of natural convection in an inclined cavity are well-illustrated in the present study.

(a)   (b)

World Academy of Science, Engineering and Technology
International Journal of Mathematical and Computational Sciences
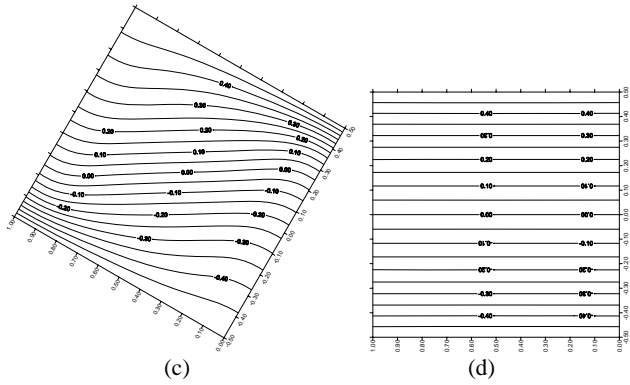Vol:2, No:10, 2008

Fig. 2 Temperature contours at $y = 0.5$ plane for $Ra = 10^5$ in a different angle (a) $\phi = 0^0$ (b) $\phi = 30^0$ (c) $\phi = 60^0$ (d) $\phi = 90^0$
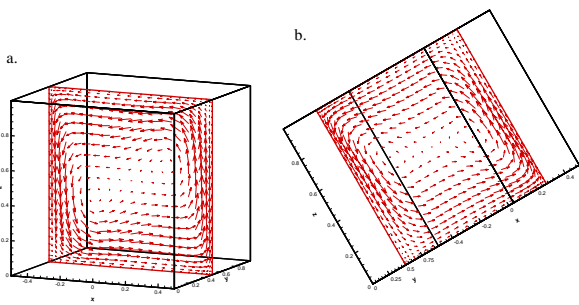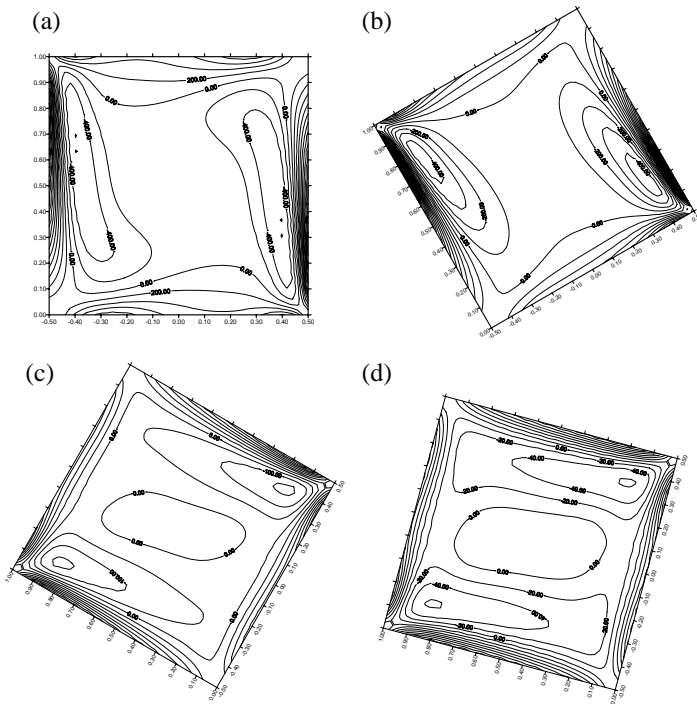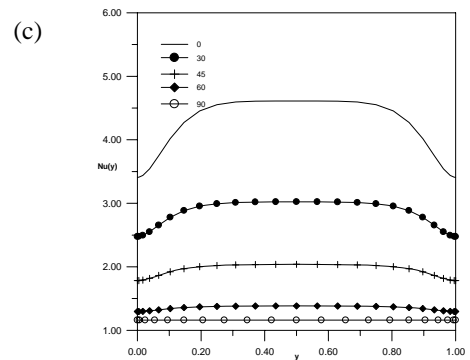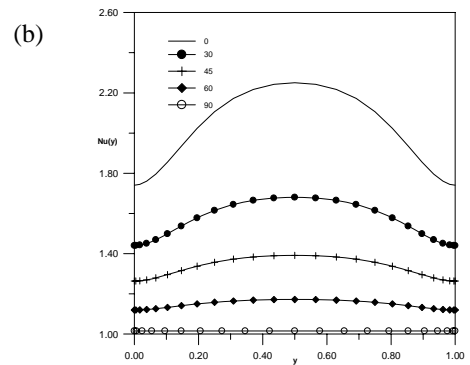
REFERENCES

[1] H. Fasel, "Investigation of the stability of boundary layers by a finite-difference model of the Navier-Stokes equations", J. Fluid Mech., 78, 1976, 355-383.
[2] R. E. Bellman, B.G. Kashef, J. Casti, "Differential quadrature: a technique for the rapid solution of nonlinear partial differential equations", J. Comput. Phys., 10, 1972, 40-52.
[3] C. Shu, Differential quadrature and its application in engineering, Springer, London, 2000.
[4] E. Tric, G. Labrosse, M. Betrouni, "A first incursion into the 3D structure of natural convection of air in a differentially heated cubic cavity, from accurate numerical solutions", Int. J. Heat Mass Transfer, 43 , 2000, 4043-4056.

Fig. 3 Velocity vectors at $y = 0.5$ plane for $Ra = 10^5$ in a different angle (a) $\phi = 0^0$ (b) $\phi = 30^0$
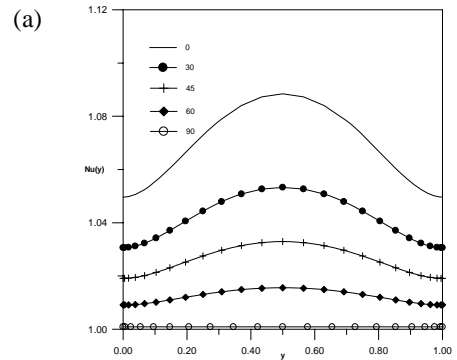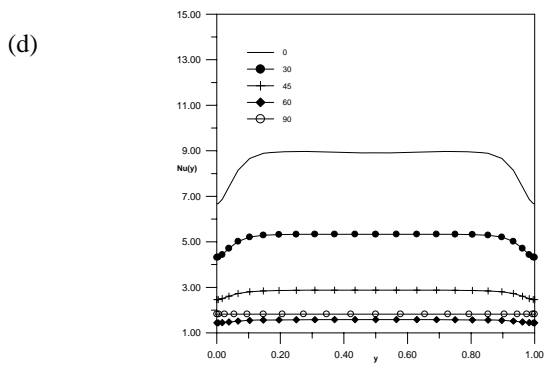

Fig. 4 Vorticity contours at $y = 0.5$ plane for $Ra = 10^5$ in a different angle (a) $\phi = 0^0$ (b) $\phi = 30^0$ (c) $\phi = 60^0$ (d) $\phi = 75^0$

World Academy of Science, Engineering and Technology
International Journal of Mathematical and Computational Sciences
Vol:2, No:10, 2008

(d)

Fig. 5 Distribution of the mean Nusselt number along the $y-$ direction for (a) $Ra = 10^3$ (b) $Ra = 10^4$ (c) $Ra = 10^5$ (d) $Ra = 10^6$